3. RESULTS

3.1. Heat-induced disassembly of the manganese complex of PSII.

In this work, the time course of the disassembly of the manganese complex using PSII membranes in solution was investigated. PSII membranes were heated to a temperature of 47 °C and keeping the sample at this temperature for 0 to 180 min. The processes initiated by this temperature jump were stopped by rapid cooling. This protocol was previously developed (Pospisil et al., 2003) for multilayers of PSII membrane particles to analyze the heat-induced changes at the Mn complex. Here a similar protocol was applied to PSII in solution.

3.1.1 Deactivation of O_2-evolution capacity by heating

The rate of oxygen evolution of heated PSII particles exposed to saturating continuous light was investigated (Figure 3.1). Using standard salt concentrations (5 mM $CaCl_2$, solid circles in Figure 3.1), 70% of inactivation is observed already after 5 min of heating. The decay of the oxygen-evolution activity is well described by three exponentials plus offset (Figure 3.1, black line). This results is similar to previous results on the respective rate constants (K_i) which account for the deactivation process are slightly smaller in PS II membranes compared to multilayer samples, as is shown in Table 3.1.

Table 3.1 Rates (K_i) and relative amplitudes (A_i) characterizing the loss of O_2-evolution due to a temperature jump to 47 °C.

Inactivation of O_2-evolution	A_1 / %	k_1 / min^{-1}	A_2 / %	k_2 / min^{-1}	A_3 / %	k_3 / min^{-1}
PSII membrane in solution	66	0.73	30	0.035		
PSII membrane multilayers	88	1.00	6	0.18	6	0.014

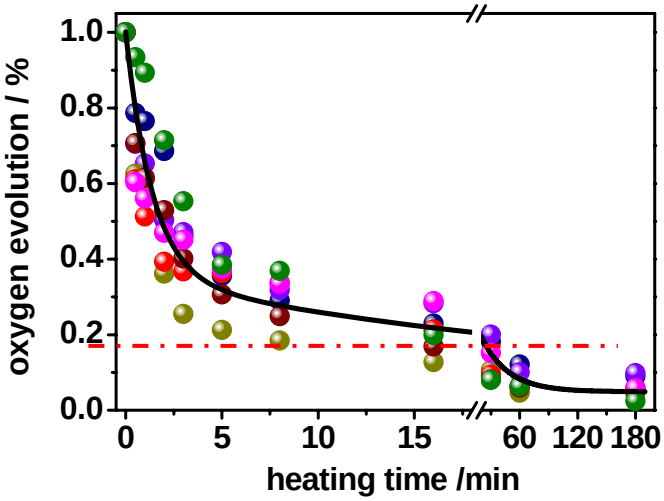

Figure 3.1 Relative oxygen-evolution activity of PSII membranes in solution previously exposed to 47 °C for various time periods. Oxygen evolution was measured in the presence of 15 mM NaCl, 5 mM $CaCl_2$, 1 M betaine, 20 mM MES-NaOH (pH 6.0), and 1 mM $K_3[Fe(CN)_6]$ plus 0.25 mM DCBQ as an electron acceptors. The black line describes the decay of the oxygen-evolution activity dominated by a rapid phase with rate constant of 0.73 min^{-1}. Data from 7 different sample series (coloured circles) were normalized to 100 % in the respective controls. (O_2-rates in the betaine-free samples were 1000-1200 µmol O_2 / mg chl x h)

3.1.2 Effects of glycinebetaine on the heat treatment

The stability of PSII membranes is largely enhanced by glycinebetaine. Because the disassembly process requires minimizing the effect of this cosolute, for all heat experiments described here, PSII particles with active OEC were prepared without betaine. The presence of betaine produces at least two effects on the PSII membrane;

1. The extrinsic polypeptides are significantly more tightly bound (Murata et al., 1992; Papageorgiou and Murata, 1995; Lee et al., 1997).
2. The inactivation of the oxygen evolution activity is moderately retarded (Williams and Gounaris, 1992; Mohanty et al., 1993; Allakhverdiev et al., 1996)

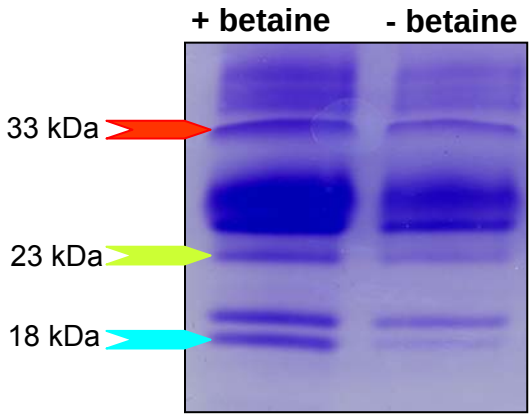

Figure 3.2 SDS of heated PSII membranes, Band (1) and (2) shows the betaine-effect on the three extrinsic polypeptides (33, 23 and 18 kDa) at 47°C.

Figure 3.2 show the stabilizing effect of betaine with respect to thermal decomposition of the PSII complex. The gel reveals that the cosolute stabilizes the three extrinsic polypeptides. This result was the first evidence that the heat-induced deactivation process may be coupled to the release of the extrinsic polypeptides from PSII.

3.1.3 Effects of the heat treatment on the extrinsic proteins.

To characterize the effect of heat treatment on the binding of the extrinsic polypeptides in greater detail, heated PSII samples were investigated by gel electrophoresis. In Figure 3.3, the region of a representative SDS gel is depicted where most of the reaction center proteins of PSII are resolvable. Visual inspection of Figure 3.3 reveals that the content of intrinsic reaction center and antenna proteins of PSII seems to be unaffected by the heat treatment.

The most pronounced effect is the rapid decrease in the intensity of the band of the extrinsic 18 KDa protein; a clearly less intense band is visible already after 2 min (Figure 3.5).

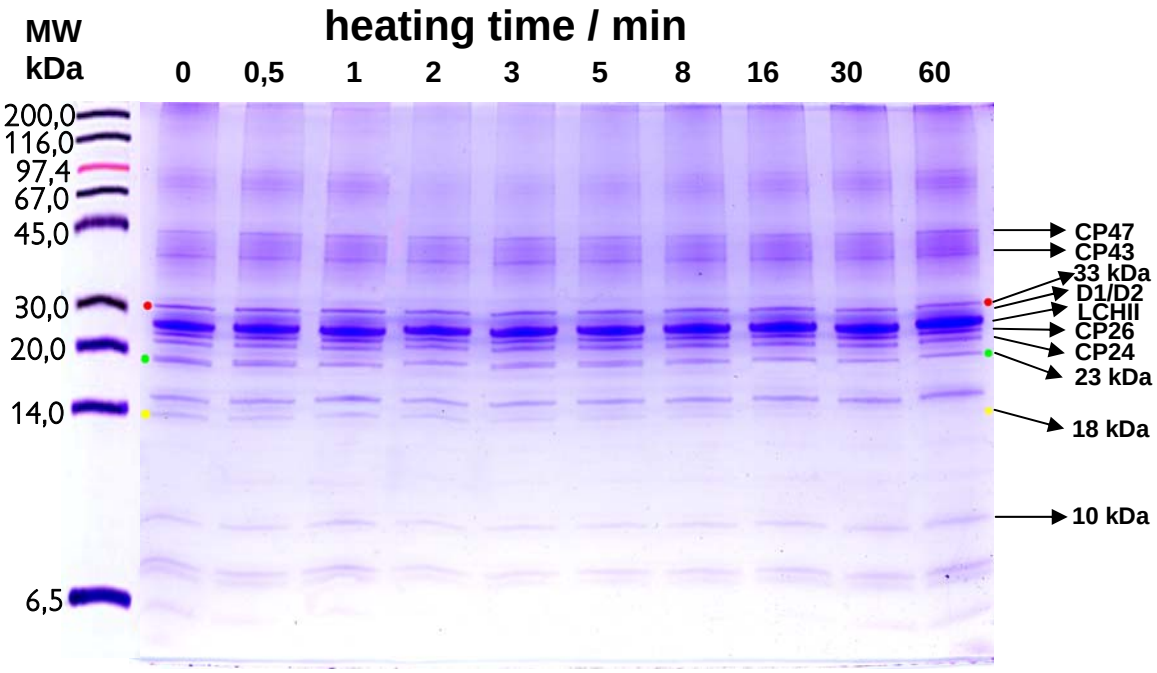

Figure 3.3 Effects of heat-treatment on the subunit composition of the PSII membranes resolved by SDS-PAGE. The red, yellow and green circles show the three extrinsic proteins; 33, 23 and 18kDa respectively. MW, masses (in kDa) deduced from molecular weight markers (MW).

Figure 3.4 shows a Western blot used to quantity the unbinding of the three extrinsic polypeptides from PSII membranes in solution by heating. A decrease of the content of the 18 kDa proteins was confirmed by immunoblotting with antibodies against the extrinsic proteins (Figure 3.4). Among the protein bands resolved, the extrinsic 18 kDa (PsbQ) was distinctly diminished at increasing heating time, whereas the 33 and 23 kDa (PsbO and PsbP respectively) showed no marked decrease.

The relative amouts of the extrinsic polypeptides in the gels were determined by scanning densitometry. The results from five different gels revealed that after 60 min of heating, the contents of the 23 and 33 KDa proteins were only slightly diminished (by about 35 and 25 %, respectively). On the other hand, the rapid loss of about 70 % of the 18 KDa protein (Figure 3.5) occurred in parallel, with almost the same rate constant (0.71 min^{-1}), to the major component of O_2-inactivation (the minor component was also similar; Table 3.1).

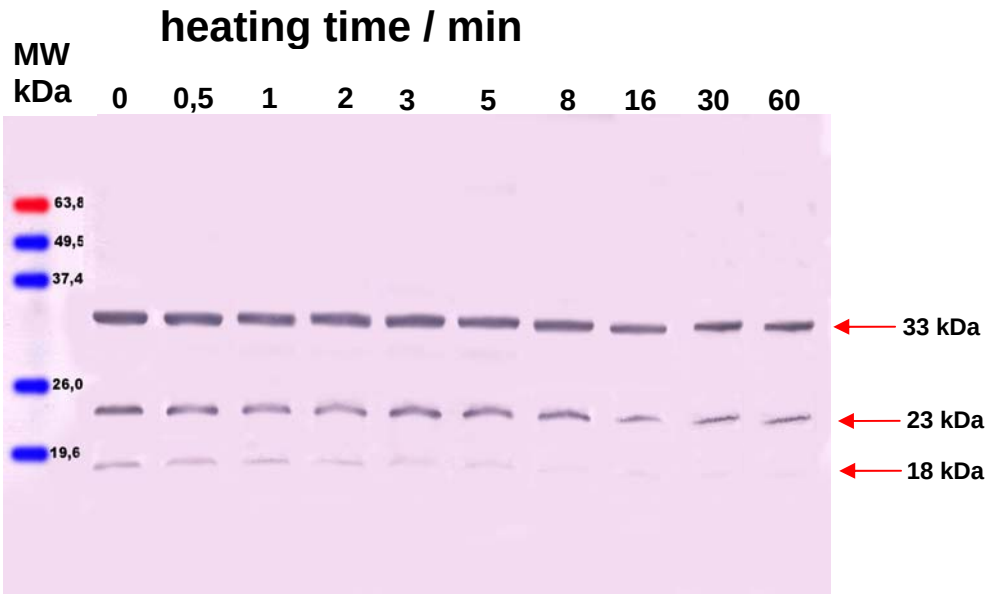

Figure 3.4. Western blot corresponding to the SDS-Gel shown in Figure 3.5. Proteins were separated by SDS-PAGE, electroblotted onto a polyvinylidene fluoride (PVDF) membrane, and probed with polyclonal antibodies (courtesy of Dr. A. Seidler, Bochum) against the three extrinsic proteins. Molecular weight markers are shown.

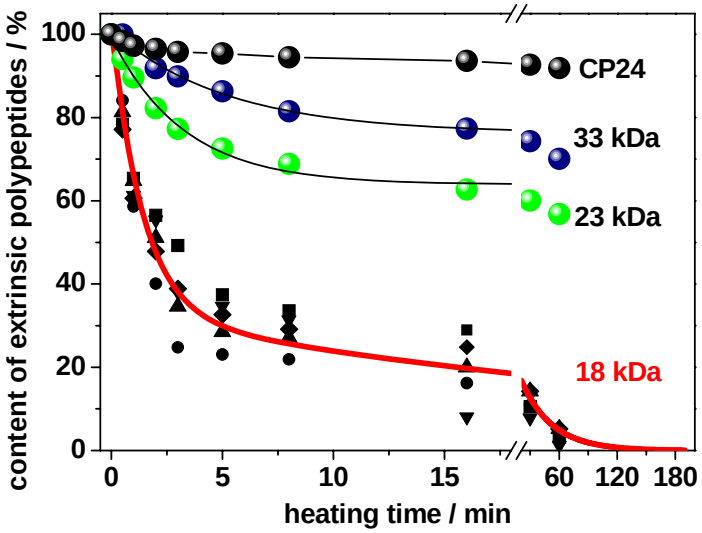

Figure 3.5 Time courses of the debinding of the three extrinsic polypeptides. The results were obtained from quantification of five different SDS-gels (for 23 and 33 kDa proteins, average values from the five gels are shown; green circles denote the CP24 protein serving as a control). Lines represent simulations (see text and Table 3-1).

At a first glance, the rapid decay of the content of the 18 kDa protein (red line in Figure 3.5.) bears a general resemblance to the decay of the oxygen-evolution activity. In order to determine whether there is a correlation between both parameters, we plotted both parameters in Figure 3.6.

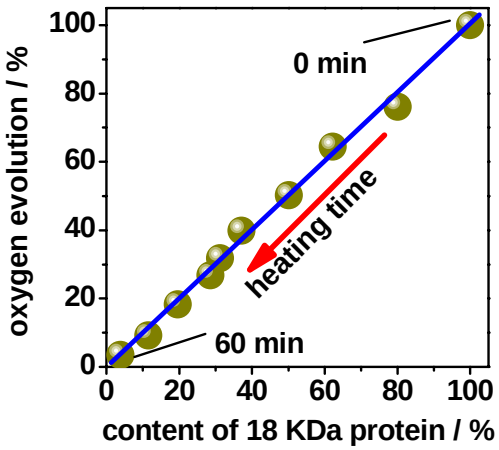

Figure 3.6 Correlation-plot of O_2-activity and content of 18 KDa protein (experimental data, dots (average of data from 5 gels and 7 data series for O_2-evolution; an offset of 4 % was subtracted from the O_2-data); line, perfect correlation).

The results show a convincing correlation between these parameters (Figure 3.6) suggesting that the loss of the 18 kDa protein may be directly related to the first step of the decay of O_2-evolution activity.

In a previous study (Pospisil et al., 2003), a kinetic model was proposed, which revealed a rapid phase (k_1 reaction) accounting for the loss of oxygen evolution, for the reduction of Y_D^{ox} and the rapid loss of calcium from PSII.

3.1.4 Delayed fluorescence experiments in heated-samples

Flash-induced delayed-chlorophyll-fluorescence transients were used as a diagnostic tool to monitor redox reactions in control PSII samples and in samples that were Ca-depleted, Mn/Ca-depleted, and heated for various time periods (Figure 3.8). (For a detailed analysis of such delayed-fluorescence transients see (Grabolle and Dau, 2005)).

In the control, the magnitudes of delayed fluorescence in the millisecond time range were small on flashes 1 and 2, large on flash 3 (Figure 3.8 A, inset), and oscillatory on higher flash numbers, reflecting electron transfer between Mn_4Ca and the Tyr_Z^{ox} with a half-decay time close to 1 ms (Karge et al., 1996) on the O_2-evolving transition (occurring for the first time on flash 3).

In Ca-depleted material (Figure 3.8 B), the ms-components were altered; relatively small on flashes 1 and 2 and larger on flash 3 and about constant on higher flash numbers. This behaviour may reflect the extraction of several electrons from Mn and Tyr_Z upon the first few flashes and charge recombination between Q_A^- and $P680^+$ on higher flash numbers (Boussac et al., 1989; Haumann et al., 1999).

In material that was depleted of both, Mn and Ca (Figure 3.8 C), delayed fluorescence differed from Ca-depleted PSII. Flash 1 revealed a smaller ms-component than the following flashes, reflecting quantitative Tyr_Z oxidation on flash 1 and charge recombination from then on (Ahlbrink et al., 1998).

Delayed fluorescence transients (not shown) of PSII membranes that were largely inactivated by heating for 4 min showed similar kinetic behaviour as the ones from Ca-depleted material (Figure 3.8 B, inset, asterisks) whereas after 60 min of heating, the kinetics more closely resembled the ones of Mn/Ca-depleted centers (Figure 3.8 C, inset, asterisks).

The rapid decay at increasing heating periods of the extent of the millisecond component attributable to electron transfer on the O_2-evolving transition on flash 3 (Figure 3.8 D) was simulated with about the same rate constant (0.75 min^{-1}) as the release of the 18 KDa protein and O_2-inactivation.

The similarity between delayed fluorescence transients from Ca-depleted and short-time heated PSII suggests that the release of the 18 KDa protein and O_2-inactivation are specifically associated with the release of Ca from the Mn_4Ca complex. Alteration of the delayed fluorescence on flash 1 in 4 min-heated PSII suggests that Ca is released already in the dark.

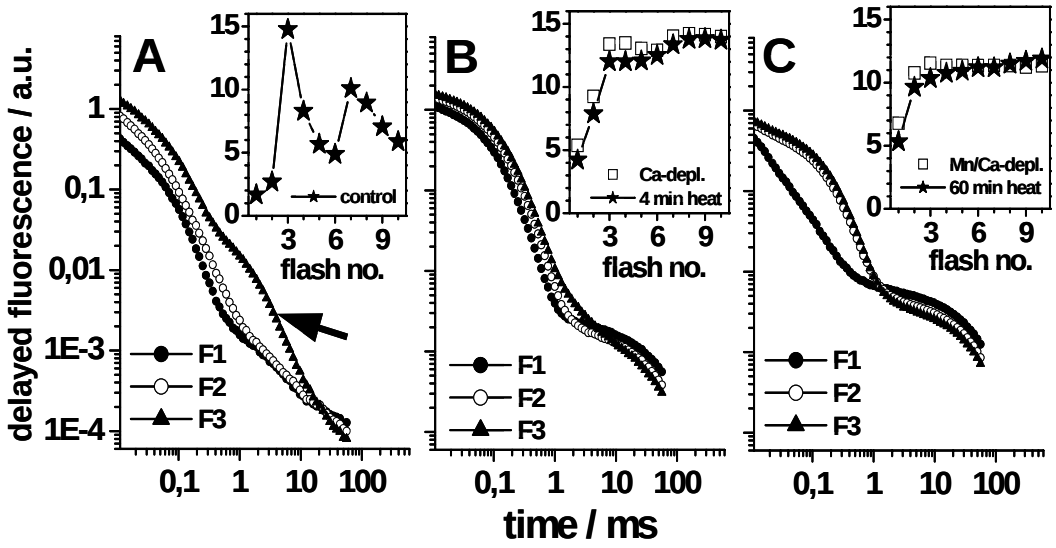

Figure 3.8: Laser-flash induced delayed fluorescence transients of PSII membranes. (A) O_2-evolving controls (Fi, flash numbers; arrow, ms-component due to electron transfer on the O_2-evolving transition). (B) Ca-depleted, (C) Mn/Ca-depleted. Main traces: decay of delayed fluorescence intensities after Laser flashes 1 to 3; insets: averages of intensities between 0.5 and 2 ms (open squares, from data as in the main traces; asterisks, from transients (not shown) of PSII membranes heated for (B) 4 min and (C) 60 min).

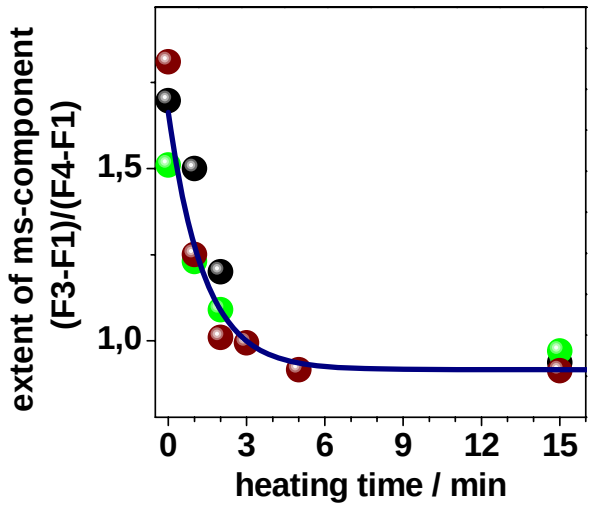

Figure 3.9 Relative extents of the millisecond phase reflecting the O_2-evolving step on flash 3 (defined as in (Messinger et al., 1993)) from heated PSII. The line represents a monoexponential decay.

The Figure 3.10 shows the laser flash-induced delayed fluorescence transients in heated PSII membranes in solution. The heat treatment affects the oscillation pattern in two ways. First, the magnitude of DF in the millisecond time range after the 3rd flash was lowered and

second, after 15 min of heating, the oscillatory behaviour after the 3rd flash was abolished. These results are in agreement with the loss of O_2-activity within short periods of heating.

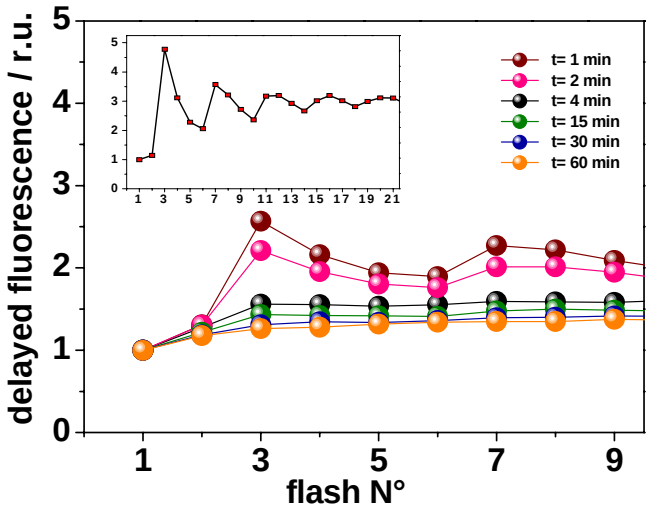

Figure 3.10 Laser flash-induced delayed fluorescence transients in heated PSII membranes in solution. As shown in the inset, DF from untreated PSII membranes in solution shows the typical flash-number dependence of dioxygen formation.

The oscillation patterns in NaCl-washed (1 M NaCl) and $CaCl_2$- washed (1 M $CaCl_2$) PSII membranes are shown in Figure 3.11.

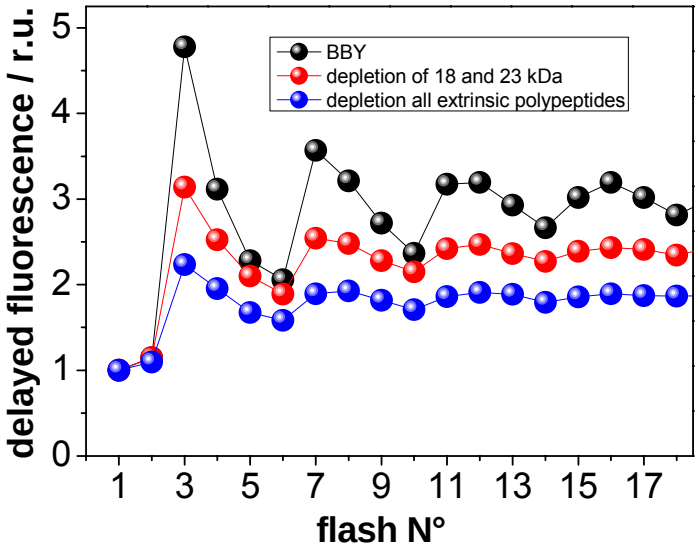

Figure 3.11 The millisecond phase of laser flash-induced delayed fluorescence transients for PSII membranes in solution after incubation with NaCl (1.0 M) and $CaCl_2$ (1.0 M). Untreated PSII membranes as control (black circles); Incubation in NaCl (1.0 M) produced the depletion of 18 and 23 kDa polypeptides (red circles) and 1 M $CaCl_2$ depleted the three extrinsic proteins (blue circles).

By NaCl washing, two peripheral proteins (18 and 23 kDa) are removed while the 33 kDa protein and all manganese atoms remain associated with the membranes, and O_2-evolution is diminished by about 50%. Whereas incubation with $CaCl_2$ (1.0 M) produced the depletion of the three extrinsic polypeptides (18, 23 and 33 kDa) the manganese atoms remain mainly bound. As shown in Figure 3.11, the oscillations were similar to the control after NaCl and $CaCl_2$ washing. However, a reduction in the DF magnitudes may be explained by the accelerated decay of the higher S-states between the flashes.

3.1.5 Manganese released monitored by EPR spectroscopy

EPR spectroscopy was employed to study the behavior of the Tyr_D^+ radical and S_2-state multiline EPR signal in heated PSII membranes samples. It has been known for a long time that tyr-161 of the D2 protein is not actively involved in the PSII electron transfer chain, but mostly is present as a radical, $Tyr_D^\bullet$ (Debus et al., 1988; Vermaas et al., 1988). $Tyr_D^\bullet$ gives rise to a narrow EPR signal centered at g = 2 (see (Miller and Brudvig, 1991)). Reduction of $Tyr_D^\bullet$ results in the disappearance of the associated EPR signal. The amplitude of the $Tyr_D^\bullet$ signal rapidly decreased with heating time and was close to zero after about 5 min (Figure 3.12, inset). The decrease of the Tyr_D^+ signal (Figure 3.12, open circles) is well described by a single exponential with the same rate constant as observed for the loss of oxygen evolution, namely 0.73 min^{-1}.

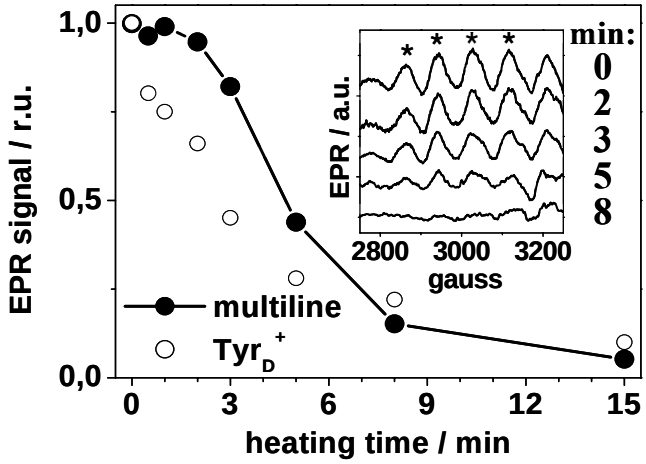

Figure 3.12 Decrease of the amplitude of EPR signals in response to heating. Solid circles, S_2-state multiline signal generated by 200 K illumination (inset: low-field region of light-minus-dark spectra; amplitudes were determined from peak-to-trough heights of lines marked by asterisks); open circles, extents of Tyr_D^+ radical signal in the same respective dark-adapted samples (from double integration of spectra, not shown). Spectra were normalized with respect to the rhombic iron signal emerging around g = 4 (not shown).

The S_2-state multiline EPR signal in samples illuminated at 200 K after heating was employed to monitor the release of Mn from its binding site subsequently to its reduction (Figure 3.12). A large multiline EPR-signal was observed in the control (Figure 3.12, inset, 0 min). For increasing heating times, the signal gradually decreases; after about 8 min it was no longer detectable. The decrease in the magnitude of the S_2-state multiline EPR signal is biphasic (Figure 3.12, line). The decrease is apparently preceded by a lag phase (Figure 3.12, line with solid circles); the stable Tyr_D^+ (tyrosine-161 on the D2 subunit) radical signal disappeared more rapidly (Pospisil et al. 2003). Loss of the 18 KDa protein may facilitate access to Tyr_D^+ from the bulk, favoring its reduction. Multiline formation in short-time heat-inactivated PS II suggests that at least one Mn oxidation can proceed in the then, presumably, Ca-depleted centres.

Heat treatment is known to result in manganese release. The six-line EPR signal from released Mn^{2+} was measured in samples of heated PSII membranes (Figure 3.13) for increasing time periods of heat treatment. As is evident from this figure, short time heat treatment did not induce the Mn^{2+} EPR signal. More prolonged heat treatment, however, results in concomitant appearance of the Mn^{2+} signal.

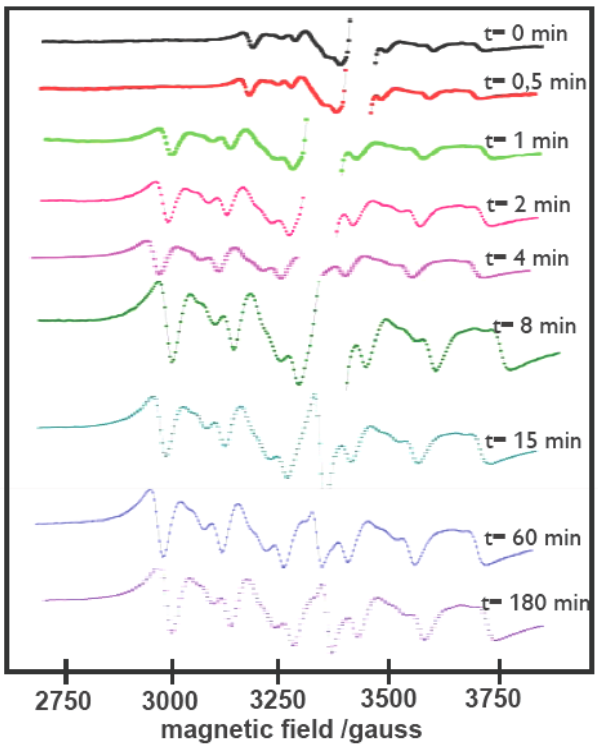

Figure 3.13 EPR spectra of Mn2+ in PSII membranes after different heating times. Measurement conditions; temperature 10 K, microwave frequency 9.1 GHz, microwave power 1 mW; modulation amplitude 2.5 G; modulation frequency 100 kHz.

3.1.6 Quantification of Mn by atomic absorption spectroscopy

To quantify the content of Mn in PSII samples previously exposed to 47 °C for various time periods, atomic absorption spectroscopy (AAS) was performed. AAS revealed that the loss of Mn to the bulk was slower than inactivation (Figure 3.14). About two Mn ions were released within ~15 min of heating. For short heating periods, there were indications for a lag phase in the Mn release. This lag was more clearly detectable in EPR-spectra (not shown) due to Mn(II) formed in the heated samples (Figure 3.14, inset). A fit of the AAS data (line) by a consecutive reaction scheme (Pospisil et al., 2003) yielded a rate of 0.13 min^{-1} for the release of the first two Mn(II) ions. The lag was described by a similar rate as O_2 inactivation.

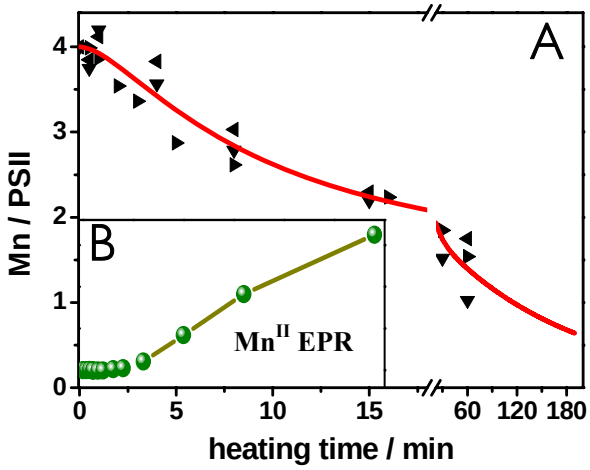

Figure 3.14 (A) Quantification of the content of Mn/PSII. The content in non-heated samples was normalized to 4. (B) Normalized magnitudes of the Mn(II) six-line EPR signal.

3.2 Assembly by photoactivation after thermally accelerated disassembly of the manganese complex of PSII.

PSII in solution was exposed to a temperature of 47 °C for increasing time intervals and thereafter the oxygen evolution activity was determined by polarography. Figure 3.15 shows that the decrease of the O_2 activity (red circles) exhibits three kinetic components as previously. The most rapid phase (rate constant k_1 = 0.8 min^{-1}) accounts for the loss of more than 60 % of the control activity. It was terminated already after about 5 min of heating. Then, O_2 activity decreased about ten times more slowly (k_2 = 0.08 min^{-1}). This phase was terminated after about 15-20 min of heating. The decrease of the remaining small offset activity of ~ 8 % was not completed (k_3 = 0.008 min^{-1}) in the time interval of 120 min of heating.

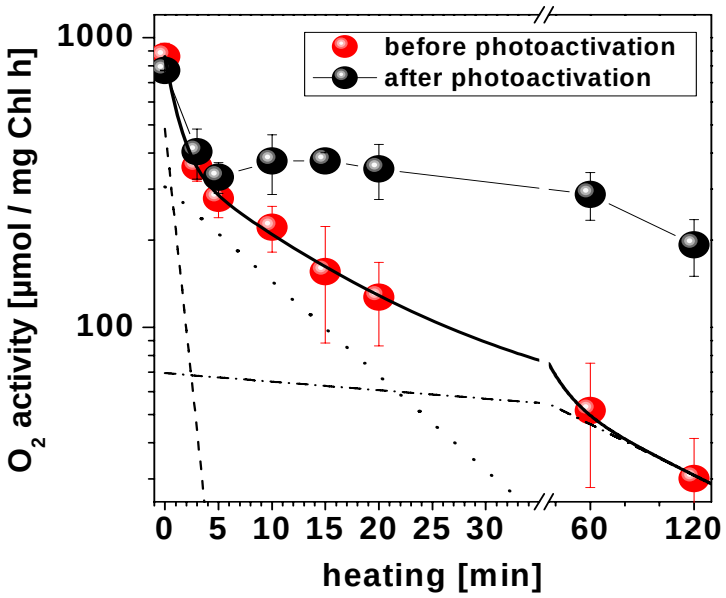

Figure 3.15 Decrease of the oxygen evolution activity of PSII membrane samples during heating to 47 °C (red circles) and activity in the same samples after subsequent photoactivation for 60 min (black circles). Three data sets were averaged. Error bars denote standard deviations (SD). The solid line represents a triple exponential simulation with parameters given in the text. Broken lines show the individual contributions of the three kinetic components.

The most rapid phase of the decrease of the O_2 activity is associated with the concomitant release of the extrinsic polypeptide with 18 kDa molecular weight from PSII (Barra et al., 2005). Already after 3 min of heating the 18 kDa protein was almost undetectable by gel electrophoresis, whereas the 23 kDa protein remained mostly bound as revealed by comparison with control PSII samples and samples in which both the 18 kDa and the 23 kDa extrinsic proteins quantitatively were removed from PSII by a NaCl-wash procedure (Figure 3.16). The second phase of the O_2 activity decrease reflects the release of two Mn ions of the Mn_4 complex as Mn(II) into the medium (see above).

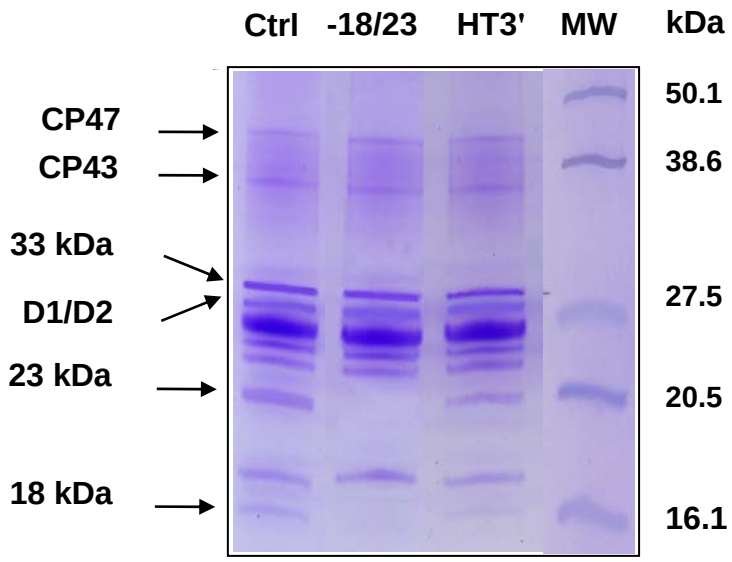

Figure 3.16 SDS gel of control (Ctrl) betaine-free PSII membranes, of samples where the extrinsic 18/23 kDa proteins were removed by a NaCl-wash treatment (-18/23), and of samples heated for 3 min (HT3´); MW, molecular weight standard.

3.2.1 Photoactivation starting at various disassembly stages.

PSII samples heated for increasing time intervals were subjected to a photoactivation procedure (see Chapter 2, Materials and Methods) for 60 min, employing weak white light illumination and the addition of approximately stoichiometric amounts of Mn^{II} per PSII reaction center (4 Mn per 200 chlorophyll) to the samples. The resulting O_2 activities are shown in Figure 3.15 as red circles. The diminished O_2 activity observed in PSII samples which were heated for less than about 5 min could not be increased by illumination. For heating intervals between 5 and 20 min, photoactivation increased the activity to an about constant value of ~400 µmol O_2 (mg chl. h)$^{-1}$. Apparently, the presence of stoichiometric amounts of

Mn(II) (and of superstoichiometric Ca^{2+}) in the photoactivation mixture was sufficient to restore the activity to a value similar to that observed in the PSII samples depleted of the 18 kDa protein by ~5 min of heating. For longer heating times up to 120 min, a similar activity was still reached after photoactivation. Clearly, the heat-treated PSII was able to serve as starting material for photoactivation.

Previous XAS studies and measurements of recombination chlorophyll fluorescence transients (the so-called delayed fluorescence, DF (Grabolle and Dau, 2005)) suggested that the loss of the 18 kDa protein in short-time (≤5 min) heated samples is accompanied by a diminished affinity of the essential Ca^{2+} ion to its binding site at the Mn complex (Pospisil et al., 2003; Barra et al., 2005). Measurements of the O_2 activity of samples heated for 3 min and subsequently photoactivated under variation of the Ca^{2+} concentration in the assay medium revealed a decreased activity in the absence of additional Ca^{2+} (i.e. at a residual Ca^{2+} concentration of about 150 µM) and an apparent activity increase by a factor of about 1.5 at an optimum concentration of 20 mM Ca^{2+} in the medium (Figure 3.17 (A)).

At higher concentrations, Ca^{2+} became inhibitory, possibly because such conditions caused the release of the 23/33 kDa extrinsic proteins in a fraction of the PSII centers (Ono and Inoue, 1984; Ananyev and Dismukes, 1996b) and/or Ca^{2+} competed with Mn for its binding sites (Chen et al., 1995; Zaltsman et al., 1997). A simple kinetic model ((Figure 3.17), see legend) involving two counteracting processes at increasing Ca^{2+} concentrations, yielded a K_D of 4.2 mM Ca^{2+} for the activating process and a half-inhibition concentration of 31.4 mM Ca^{2+}. The maximal O_2 activity of ~800 µmol (mg chl. h)$^{-1}$, which would be reached by the Ca^{2+}-dependent activation in the absence of an inhibitory effect was similar to the unheated controls (dotted line in Figure 3.17 (A)). These results strengthen our previous notion (Pospisil et al., 2003; Barra et al., 2005) that the diminished affinity for Ca^{2+}, likely brought about by the loss of the 18 kDa protein, is the primary cause for the lowered O_2 activity in short-time heated PSII.

EXAFS measurements at the Mn K-edge have revealed that after about 15-20 min of heating a binuclear Mn complex is formed in which the two Mn ions are still connected by a di-µ-oxo bridge (Pospisil et al., 2003; Barra et al., 2005). As clearly visible in (Figure 3.15), PSII samples heated for 15-20 min could be photoactivated. The reached activity was similar to that in samples heated for less than 5 min. The straightforward interpretation of this result is that the Mn_2 complex formed after 15-20 min of heating can serve as a starting state in the photoactivation process. The maximal achievable activity depends on the light intensity during photoactivation (Figure 3.17 (B)).

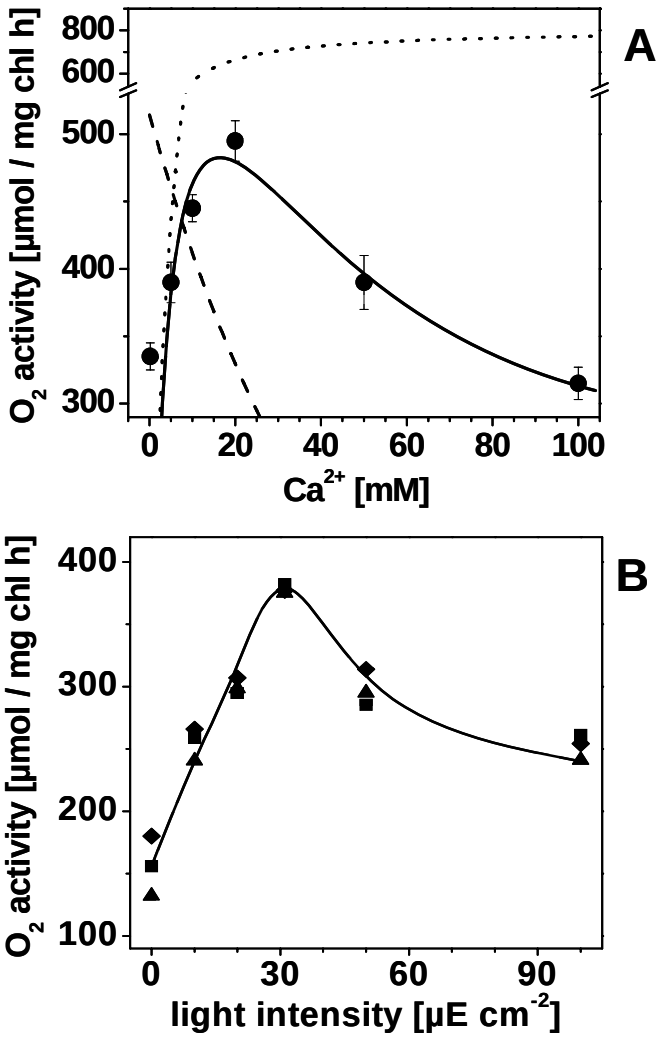

Figure 3.17 (A) O_2 activity of PSII membranes heated for 3 min (solid circles) as a function of the Ca^{2+} concentration in the assay medium. Three data sets were averaged; error bars denote SD. The solid line represents a simulation using the following equation to describe the O_2 activity: $O_2 = O_2^{max}$ $[Ca^{2+}]$ / (K_M + $[Ca^{2+}]$) – O_2^{min} [1-exp(-ln(2) $[Ca^{2+}]$ / $[Ca^{2+}]_{1/2}$)]. The broken lines show the contributions of the two counteracting processes. (B) O_2 activity in PSII membranes heated for 15 min and subsequently photoactivated for 60 min at the indicated light intensities. Three data sets are shown; the line has been drawn to guide the eye.

Optimum activities after photoactivation of samples heated for 15 min (and also for 120 min, not shown) were observed at ~30 µE m^{-2}. For photoactivation after Mn depletion, similar optimum light intensities have been reported (Tamura and Cheniae, 1987; Tamura et al., 1989; Chen et al., 1995). After 120 min of heating, most Mn ions were released from PSII as Mn(II). Clearly, the thereby formed apo-PSII was also functional in photoactivation (Figure 3.15).

3.2.2 Kinetics of photoactivation in previously heated samples

We explored the time course of the photoactivation process in PSII samples which were exposed previously to the heat-treatment. The O_2 activity in 3 min heated PSII was about independent of the photoactivation time (Figure 3.18, triangles), in line with the absence of Mn release from short-time heated PSII. In samples heated for 15 min, on the other hand, the activity increased during the photoactivation and reached a constant level after about 40 min (Figure 3.18, circles).

The increase was well described by a single-exponential function with a rate constant k_{A2} = 0.095 min^{-1} (line). In samples heated for 120 min, the increase in activity was not monophasic. Rather, during the first 5 min of photoactivation, a lag phase (arrow) was observed during which the activity remained low, and only thereafter, an apparently monophasic activity increase occurred (Figure 3.18, squares). Such a time course suggested that the photoactivation involved at least two sequential steps. Indeed, using a consecutive reaction scheme (Pospisil et al., 2003) and employing an apparent rate constant of k_{A1} = 0.25 min^{-1} ($t_{1/2}$ = 2.8 min) to account for the lag phase and the above rate of k_{A2} = 0.095 min^{-1} ($t_{1/2}$ = 7.3 min) for the monophasic increase yielded a satisfying description of the data points (Figure 3.18, solid line). Monitoring photoactivation in samples where Mn depletion was achieved by a reductive treatment in the presence of hydroxylamine (NH_2OH) followed by a washing step to remove the liberated Mn(II) ions revealed that the lag-phase behavior was not a specific property of the long-time heated PSII, but observable also in apo-PSII samples produced by reductive Mn removal (Figure 3.18, asterisks).

In summary, the time course of the photoactivation suggests that, when apo-PSII with an unoccupied Mn binding site is employed as the starting material, within ~5 min an intermediate state of the Mn complex is formed, which is inactive in O_2 evolution. Subsequently, in a slower reaction the functional Mn_4 complex is assembled. Both steps require the input of light energy. When the presumably binuclear Mn complex (see below) is used as the starting point, photoactivation to yield the Mn_4 complex occurs without a lag phase. These results can be explained by assuming that the intermediate formed after ~5 min of photoactivation of apo-PSII corresponds to the same binuclear Mn complex that is formed in the disassembly process after ~15 min of heating.

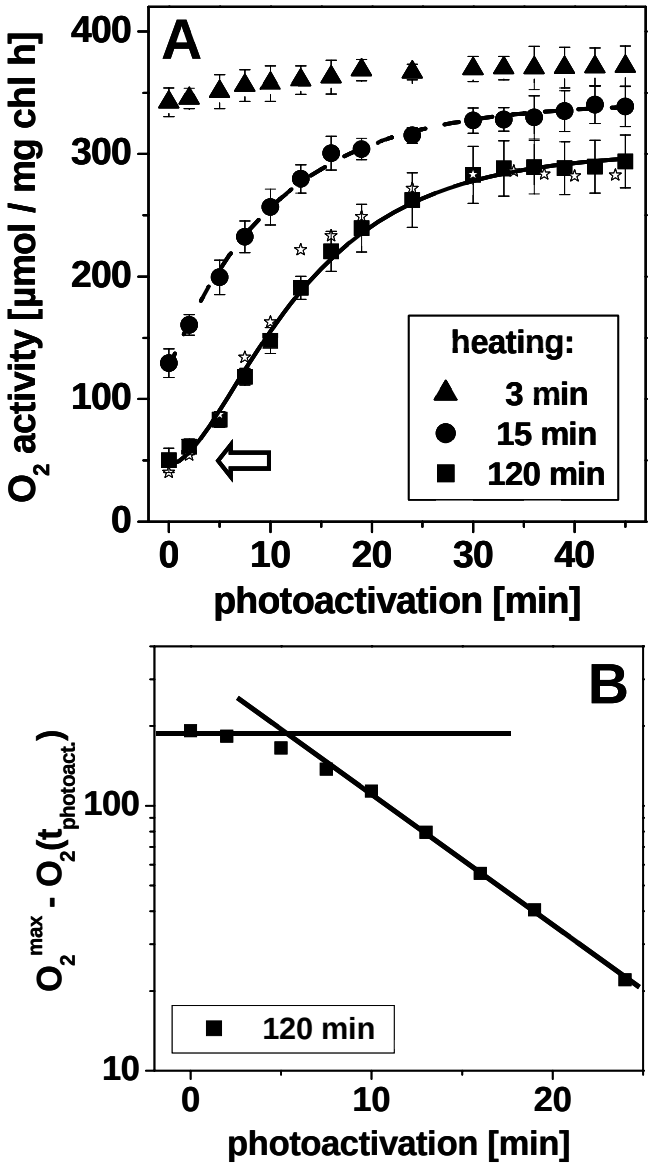

Figure 3.18 (A) Time courses of photoactivation after previous heat-deactivation for the indicated time periods. The data points represent the average of three experiments (error bars denote SD). Dashed line, single exponential simulation; solid line, simulation using a consecutive reaction scheme (Pospisil et al., 2003), for parameters see text. Asterisks denote activities measured on samples that were depleted of the 18/23 kDa extrinsic proteins by a NaCl-wash procedure, then depleted of Mn/Ca by reduction with hydroxylamine (NH_2OH), and subsequently photoactivated. The arrow points to the lag phase of ~5 min duration in the recovery of O_2 activity. (B) Semilogarithmic plot of the data for 120 min photoactivation. Lines have been drawn to emphasize the deviation from the linear behavior which is expected in the absence of a lag phase.

3.2.3 Mn requirement for reassembly of the Mn_2-complex

In samples heated for 15 min, the release of two of the four Mn ions of the complex as Mn(II) to the suspending medium has been observed. Two Mn ions remain bound to PSII (Pospisil et al., 2003; Barra et al., 2005). Such samples were subjected to the photoactivation procedure in the absence of additional Mn, meaning that the two bound ions and the two ions released into the medium were still present. The initial activity of these samples increased monophasically during photoactivation (Figure 3.19, solid symbols) to a value that was similar to that of samples heated for only 3 min (Figure 3.18), which contain four Mn ions bound to PSII. Seemingly, the liberated MnII ions were reincorporated into the complex during photoactivation so that the O_2-evolving Mn_4 site was recovered to almost 100 %. When the 15 min heated samples were washed subsequently to remove all unbound or loosely bound Mn ions, photoactivation was not possible without adding Mn (Figure 3.19, asterisks).

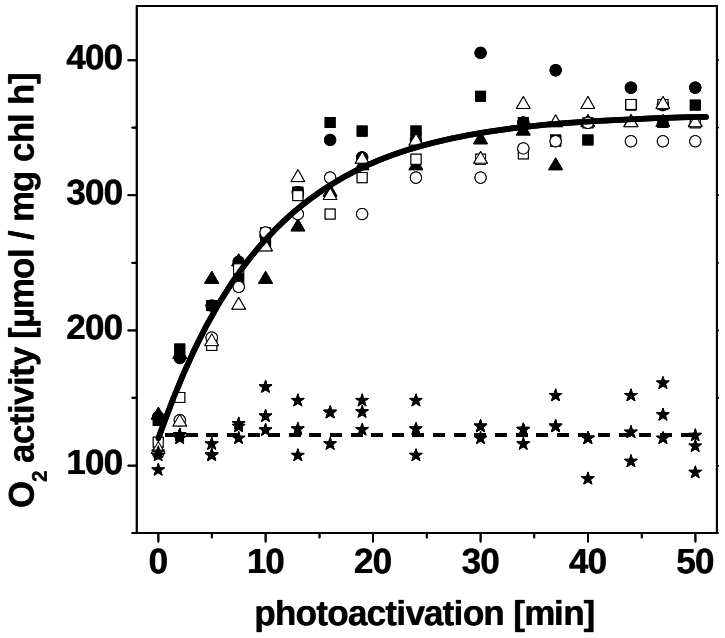

Figure 3.19 Time courses of the recovery of O_2 activity during photoactivation in PSII samples previously heated for 15 min. Solid symbols, three data sets from PSII samples that, after heating, were photoactivated in the absence of additional Mn; open symbols, one washing step after heating to remove unbound Mn, and subsequent photoactivation after the addition of 2 Mn^{II} ions per PSII to the medium; asterisks, one washing step after heating to remove unbound Mn and photoactivation without additional Mn. The solid line represents a single exponential simulation with k_{A2} = 0.095 min^{-1}.

Thus, there was no detectable redistribution of the two bound Mn ions among the PSII reaction centers. However, activity was almost fully recovered, when two Mn(II) ions per PSII

reaction center were added to the photoactivation medium after washing (Figure 3.19, open symbols). The two Mn ions remaining after 15 min of heating are bound relatively firmly to PSII, in agreement with previous observations (Pospisil et al., 2003; Barra et al., 2005).

3.2.4 Stability of the Mn_2-intermediate of photoactivation.

The stability of the state that has been formed after only 5 min of photoactivation (i.e. during the lag-phase, see (Figure 3.18) was studied, starting with apo-PSII created by 2 h heating and subsequent washing to remove the liberated Mn ions. Such PSII membranes were photoactivated for 5 min in the presence of 2 Mn per PSII center, thereafter incubated for increasing time intervals in the dark, and subsequently photoactivated for 40 min. The resulting O_2-activities are depicted in Figure 3.20 (circles). Up to a duration of about 15 min of the intervening dark interval, the final activity remained low (at its background level), but for longer dark intervals increased by a value (~120 µmol O_2 (mg chl. h)$^{-1}$) that was about half of the increase obtained after photoactivation with 4 Mn per PSII center (~240 µmol O_2 (mg chl. h)$^{-1}$, dashed line).

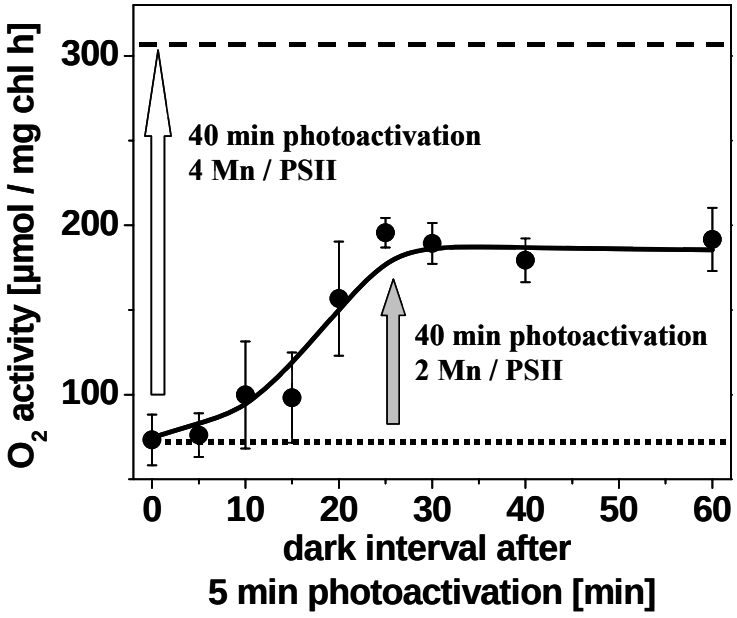

Figure 3.20 Final O_2-activities in PSII membranes photoactivated for 5 min with 2 Mn per PSII at increasing intervals of dark incubation on ice prior to the final photoactivation for 40 min (circles). The dashed line represents the activity after photoactivation with 4 Mn per PSII. For further details see text.

The above results suggest that the two Mn ions that become bound to PSII within 5 min of photoactivation remain bound for ~15 min in the dark (and also for 40 min in the light). For longer dark-exposure times, these two Mn ions are released, possibly cooperatively, to the

medium. Only after this Mn release, centers with 4 Mn are formed in about half of the PSII population in the subsequent 40 min photoactivation procedure. If the PSII membranes were collected by centrifugation after 5 min of photoactivation with 2 Mn per PSII, resuspended, and supplied with additional 2 Mn per PSII center (duration of the whole procedure ~15 min), and then photoactivated for 40 min, the gain in activity was about 70 % (~180 µmol O_2 (mg chl. h)$^{-1}$) of that obtained after photoactivation with 4 Mn per PSII. Besides providing insights into the stability of the Mn_2 intermediate, these findings open up the way to spectroscopic studies, which will be described below.

3.2.5 DF measurements confirm intermediate formation.

The formation of a partially assembled Mn complex after only 5 min of photoactivation may suggest that the bound Mn could function as an electron donor to the oxidized tyrosine-Z (Y_Z^{ox}) formed upon flash excitation of the sample (Miller and Brudvig, 1990; Ahlbrink et al., 1998; Barra et al., 2005). This option was explored by measurements of the decay of delayed chlorophyll fluorescence (DF) (Clausen et al., 2005; Grabolle and Dau, 2005) after laser flash excitation (Figure 3.21). Prior to photoactivation, i.e. in the absence of bound Mn, the DF transient on flash 1 decayed more rapidly than on the following flashes (Figure 3.21 (A), 0 min) as expected for oxidation of Y_Z by $P680^+$ only on flash 1 in tens of microseconds (Ahlbrink et al., 1998; Barra et al., 2005) and charge recombination between $P680^+$ and Q_A^- occurring on the following flashes in the hundreds of microseconds time range (Ahlbrink et al., 1998; Barra et al., 2005). During the first few minutes of photoactivation, there was a decrease in the DF amplitude induced by flash 1 in the milliseconds time range (Figure 3.21 (A), 7.5 min), but the DF transients on higher flash numbers were almost unchanged. Accordingly, on the higher flashes, charge recombination still was the dominating process. However, the decreased DF amplitude on flash 1 is compatible with partial reduction of Y_Z^{ox} by the Mn_2 complex on the milliseconds time scale. After 50 min of photoactivation, there was a pronounced DF phase with a decay half-time of ~1.1 ms on flash 3 (Figure 3.21 (A), 50 min). This phase is related to Y_Z^{ox} reduction during O_2-formation on transition $S_3 \rightarrow S_0$ as previously shown (Clausen et al., 2005; Haumann et al., 2005a).

Figure 3.21 (B) shows the mean DF amplitudes as obtained by averaging from 2 to 10 ms after each flash in samples photoactivated for increasing time intervals. Even after 50 min of photoactivation and a subsequent dark-interval of only about 1 min prior to the measurements, PSII seems to be almost dark-adapted prior to the laser flashes. The Mn complex predominantly was in its S_1-state, as there is a pronounced quaternary oscillation in the DF amplitudes related to the O_2-evolving step first occurring on flash 3. As shown in

Figure 3.21 (C), the ms-amplitude measured after the first flash decreases within the first 10 min of photoactivation possibly due to electron transfer from the Mn_2 intermediate as discussed above.

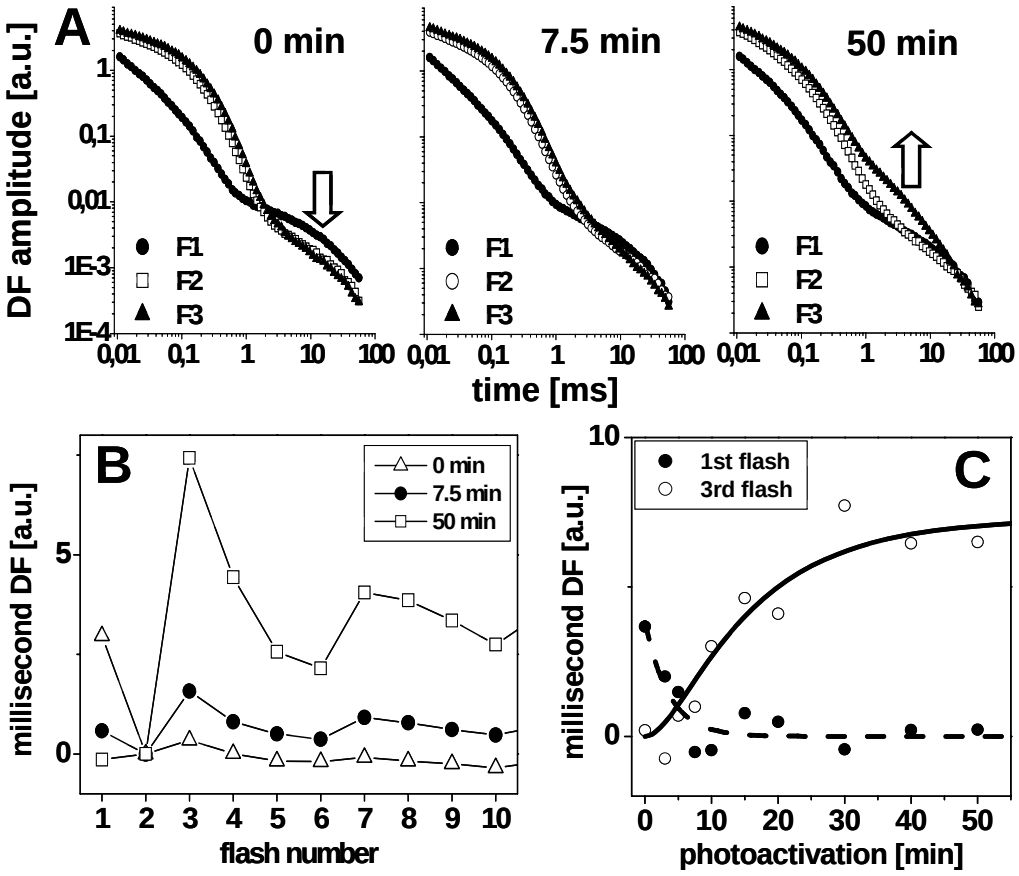

Figure 3.21 Results of delayed chlorophyll fluorescence (DF) measurements on heated and photoactivated PSII. (A) DF transients measured after illumination by one, two, or three laser flashes applied to apo-PSII samples that previously have been photoactivated for 0, 7.5, and 50 min in the presence of 4 Mn / PSII. The arrows denote the kinetic phases that decreased in amplitude on flash 1 and increased on flash 3 at increasing photoactivation period. Three transients from independent samples were averaged on each flash. (B) Mean DF amplitudes from averaging between 2 and 10 ms after each flash in a series. The three data sets have been normalized to zero on the DF-amplitude on flash 2. (C) The DF amplitudes in the millisecond time range as function of the duration of photoactivation on flash numbers 1 (solid circles) and 3 (open circles). From all DF amplitudes, a small offset value needed to set the transient on the 2nd flash of the series to zero, was subtracted. The dashed line represents a single-exponential decay with a time constant $k_{A1'}$ = 0.27 min^{-1}, the solid line was derived from a simulation using a consecutive reaction scheme, the above value of $k_{A1'}$, and $k_{A2'}$ = 0.073 min^{-1}, respectively.

The amplitude of the O_2-phase measured after the third flash may exhibit a lag-phase prior to its rise. The lag phase duration was similar to that observed in the increase of O_2-activity during photoactivation (see Figure 3.18) and confirms intermediate formation. Apparently, the amplitude decrease on flash 1 ($k_{A1'}$ = 0.27 min^{-1}) was completed within the duration of the lag phase observed for the flash 3 signal. The amplitudes on flash 3 were well simulated using the consecutive reaction scheme (Pospisil et al., 2003) and the same rate constant $k_{A1'}$ to account for the lag and a rate $k_{A2'}$ = 0.073 min^{-1} accounting for the rise (Figure 3.21 (C),

lines). The obtained rate constants, within error, are similar to those obtained from the O_2 evolution measurements (see Figure 3.18).

In conclusion, the DF results support the notion that an intermediate is formed within the first few minutes of the photoactivation process. This intermediate may be able to donate an electron to the $Y_Z^{\bullet+}$ radical.

3.2.6 X-ray absorption spectroscopy

X-ray absorption spectra at the Mn K-edge were measured on samples, which were heated and subsequently photoactivated in the presence of stoichiometric amounts of Mn (Figure 3.22). Control PSII (no heating, no photoactivation) showed a XANES spectrum (Figure 3.22 (A), thick line) that, as judged by the K-edge energy of 6551.4 eV, can be attributed to the Mn complex in its dark-stable S_1 state (Dau et al., 2004). Apo-PSII that was photoactivated for 40 min in the presence of 4 Mn per PSII (and thereafter active in O_2-evolution) and collected by centrifugation showed a similar shape of the XANES spectrum (Figure 3.22 (A), dashed line) and a slightly lower edge energy of 6551.1 eV, still compatible with the predominant presence of the S_1 state and admixtures of minor portions of lower oxidation states of the Mn_4 complex and of aqueous Mn(II). In both samples, the Mn complex seems to be predominantly present in its mean oxidation state of +3.5 of the S_1 state assignable to a $Mn(III)_2Mn(IV)_2$ complex (Dau et al., 2004; Sauer and Yachandra, 2004). The XANES spectrum of hexaquo Mn(II) ($[Mn(II)(H_2O)_6]^{2+}$ complex) is shown for comparison in Figure 3.22 (A), open circles, E_{edge} = 6547.2 eV. Samples that were heated for 15 min and subsequently washed to remove unbound Mn displayed a XANES spectrum (Figure 3.22 (A), triangles), which may be attributable to Mn(III) (E_{edge} = 6550.1 eV). This estimate is based on an edge shift of -0.6 to -0.8 eV per single-electron reduction of the Mn_4 complex initially in its S_1 state (Iuzzolino et al., 1998; Haumann et al., 2005b). Hence, the binuclear Mn complex formed after 15 min of heating may be presumably in the $Mn(III)_2$ oxidation state, in accordance with previous estimates (Pospisil et al., 2003). Samples that were heated for 120 min, washed to remove unbound Mn, subsequently photoactivated in the presence of 2 Mn per PSII for only 5 min, that is for the duration of the lag-phase observed in the photoactivation time course see Figures (3.18 and 3.21), and collected by centrifugation, displayed a XANES spectrum (Figure 3.22 (A), solid circles, E_{edge} = 6549.6 eV) which is also compatible with a major contribution from Mn(III). A minor, but significant contribution of Mn(II), accounting for the relatively low edge energy is apparent from the larger primary maximum of the edge. Such a Mn^{II} contribution was expected, and is also visible in the EXAFS spectrum (see below), because the intermediate formed after 5 min of photoactivation

showed only limited stability (compare Figure 3.20) and was partly degraded during collection of the PSII membranes by centrifugation and preparation of the EXAFS samples.

Figure 3.22 (B) (dots) shows the Fourier-transforms (FTs) of EXAFS spectra from samples previously heated for 2 h, washed, and then collected by centrifugation after photoactivation for 40 min with 4 Mn per PSII (top) or for 5 min with 2 Mn per PSII (bottom). The top spectrum revealed two major peaks (I and II) as typical for the Mn complex of PSII (Kirby et al., 1981; George et al., 1989; Sauer and Yachandra, 2004; Haumann et al., 2005b). Peak I is attributable to direct O/N ligands to Mn, peak II mainly reflects Mn-Mn distances of about 2.7 Å length (Haumann et al., 2005b). A simulation of the spectrum employing three shells of backscatterers (two O/N shells to account for the complex distance distribution in the first coordination sphere of Mn (Dau et al., 2004; Haumann et al., 2005b) and one Mn-Mn vector of ~2.7 Å length) yielded a result (Table 3.2) that was similar to previous ones obtained from simulations of EXAFS spectra of the native Mn complex in its S_1-state (Dau et al., 2004; Haumann et al., 2005b). Longer Mn-Mn/Ca vectors (Dau et al., 2003; Pospisil et al., 2003; Dau et al., 2004) were neglected because of the sizable noise level of the spectra due to a comparably low Mn concentration of ~140 µM in 40 min photoactivated samples and of ~45 µM in 5 min photoactivated samples, as estimated from the X-ray fluorescence counts due to Mn. Thus, the overall structure of the functional Mn complex created by photoactivation in vitro and of the native Mn complex appears to be similar, as expected. In particular, there is about one Mn-Mn vector of ~2.7 Å length per Mn ion ($N_{Mn\text{-}Mn}$ close to unity) in the both cases, meaning that at least two pairs of Mn ions, which each are connected by a di-µ-oxo bridge are present (Dau et al., 2003; Pospisil et al., 2003; Dau et al., 2004; Haumann et al., 2005b). The fact that the value of $N_{Mn\text{-}Mn}$ exceeded unity is attributable to the neglected Mn-metal distances larger than ~2.7 Å in the simulation approach (Dau et al., 2004; Haumann et al., 2005b).

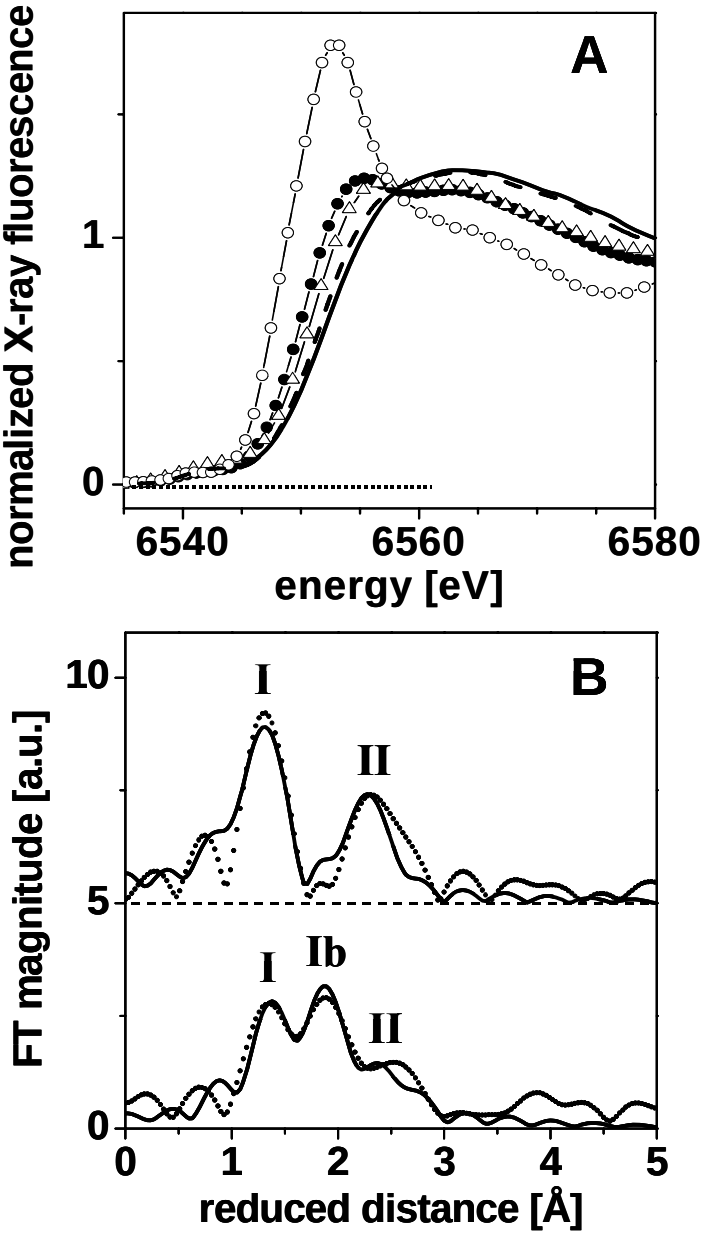

Figure 3.22 (A) XANES spectra at the manganese K-edge. Solid line, control PSII with the Mn complex in its S_1 state (no heating, no washing, no photoactivation); open circles, PSII samples heated for 2 h (no washing, no photoactivation); dashed line, samples photoactivated for 40 min with 4 Mn per PSII; open triangles, samples heated for 15 min and subsequently washed to remove unbound Mn (no photoactivation); solid circles, samples heated for 2 h, washed to remove unbound Mn, photoactivated for 5 min in the presence of 2 Mn per PSII. (B) Fourier-transforms (FTs, dots) of k^3-weighted EXAFS oscillations of samples photoactivated for 40 min with 4 Mn / PSII (top) and for 5 min with 2 Mn / PSII (bottom). FTs were calculated using a *k*-range of 2.1-11.2 $Å^{-1}$ and cosine windows extending over 10 % of the *k*-range at high and low *k*-values. Solid lines represent simulated spectra calculated with parameters in Table 3.2. In (B) spectra are vertically displaced by 5 units for better comparison.

In the spectrum of samples, which have been photoactivated for only 5 min with 2 Mn per PSII, three FT peaks are apparent (Figure 3.22 (B), bottom). The new peak Ib, according to the simulation results (Table 3.2), is attributable to Mn^{II} in water (typical Mn-O(H_2) distance of about 2.18 Å. The Mn(II) contribution also was inferred from the XANES spectrum. More interesting is the presence of Mn-Mn distances in the range of 2.7-3 Å length (peak II).

Table 3.2 Simulation results of a joint-fit (Pospisil et al., 2003) of the two EXAFS spectra shown in Figure 4.8 (B) N_i, coordination number; R_i, Mn-ligand distance; $2\sigma^2$, Debye-Waller parameter. The following restraints have been used in the simulations: The sum of the two N_{Mn-O} values was set to 5.5 and the two R_{Mn-O} and $2\sigma^2_{Mn-O}$ values were coupled in the simulation to yield the same values for both spectra. For both spectra the same fixed value of $2\sigma^2_{Mn-Mn}$ was employed. The R_F-value (error sum (Meinke et al., 2000)) of the joint fit was 37 %, calculated over a reduced distance range of 1 - 3 Å.

shell:	Mn-O	Mn-O	Mn-Mn
sample:	N_i / R_i / $2\sigma^2_i$ [per Mn / Å / Å^2]		
40 min photoactivation, 4 Mn	4.8 / 1.85 / 0.018	0.7 / 2.18 / 0.018	1.1 / 2.73 / 0.006
5 min photoactivation, 2 Mn	3.1 / 1.85 / 0.002	2.4 / 2.18 / 0.002	0.8 / 2.74 / 0.006

Simulations revealed that the number of ~2.7 Å distances per Mn ion was reduced (by at least 30 %) compared to the 40 min photoactivated samples. We note that, due to the low Mn concentrations, the data quality was relatively low so that the coordination-number value is highly uncertain. In any event, the data is compatible with the presence of a significant fraction of centers containing Mn ions connected by a di-μ-oxo bridge. Longer Mn-Mn distances may also be present, resulting from Mn ions connected by a mono-μ-oxo bridge or by di-μ-OH bridges due to partial degrading of the intermediate, which were not analysed further. Thus, the results of the polarographical photoactivation studies and XAS data analysis suggest formation of a binuclear Mn complex within the first few minutes of photoactivation. This complex may contain a $Mn(III)_2$(di-μ-oxo) motif. A similar site is formed after 15 min of heat treatment as shown in (Pospisil et al., 2003). This binuclear center may represent a relatively stable intermediate both in the thermally induced disassembly and in the photoactivation process of the Mn complex.